

Supplementary Information

A trade-off-free fluorosulfate-based flame-retardant electrolyte additive for high-energy lithium batteries

Jimin Oh^a, Ho Seung Lee^b, Min Pyeong Kim^b, Young-Gi Lee^a, Sung You Hong^{b,*}, and Kwang Man Kim^{a,*}

^a*ICT Creative Research Laboratory, Electronics and Telecommunications Research Institute (ETRI), Daejeon 34129, Republic of Korea*

^b*Department of Chemistry, Ulsan National Institute of Science and Technology (UNIST), Ulsan 44919, Republic of Korea*

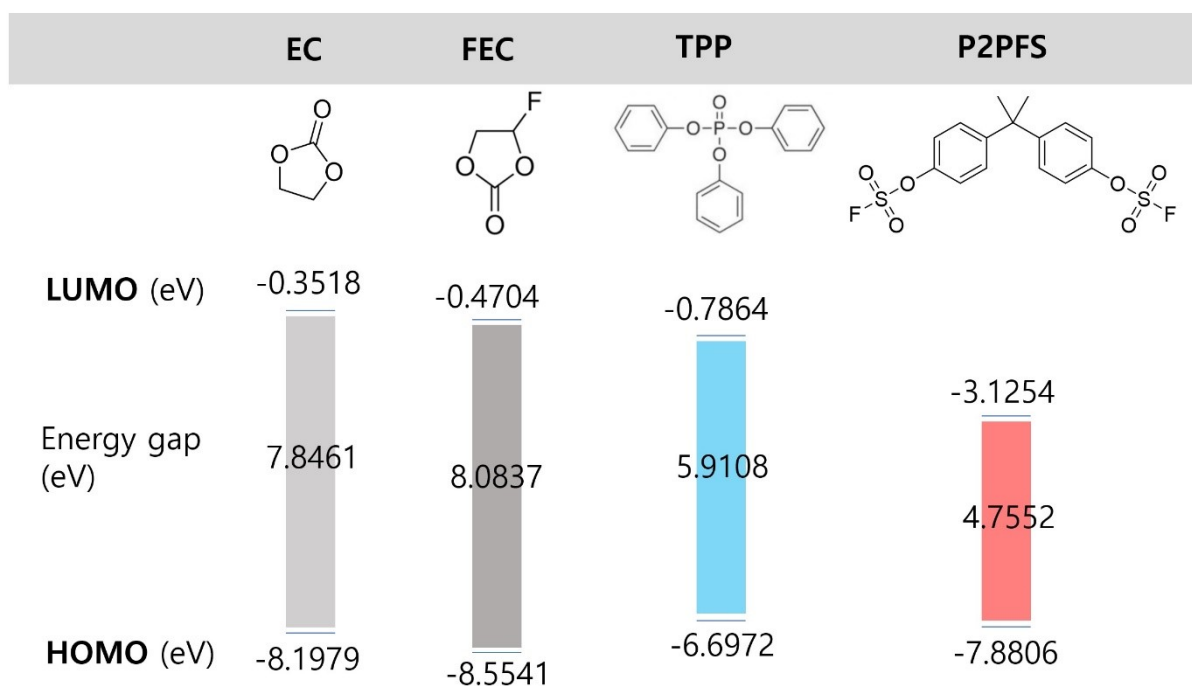


Fig.S1 Summary of HOMO-LUMO energy levels of electrolyte components and additives used in this study. Fermi molecular orbital levels were estimated by density functional theory (DFT) calculations with B3LYP hybrid functional and 6-31G(d,p) basis set. Using this set, LUMO-HOMO levels of EC were calculated as nearly similar values reported in a previous report.¹

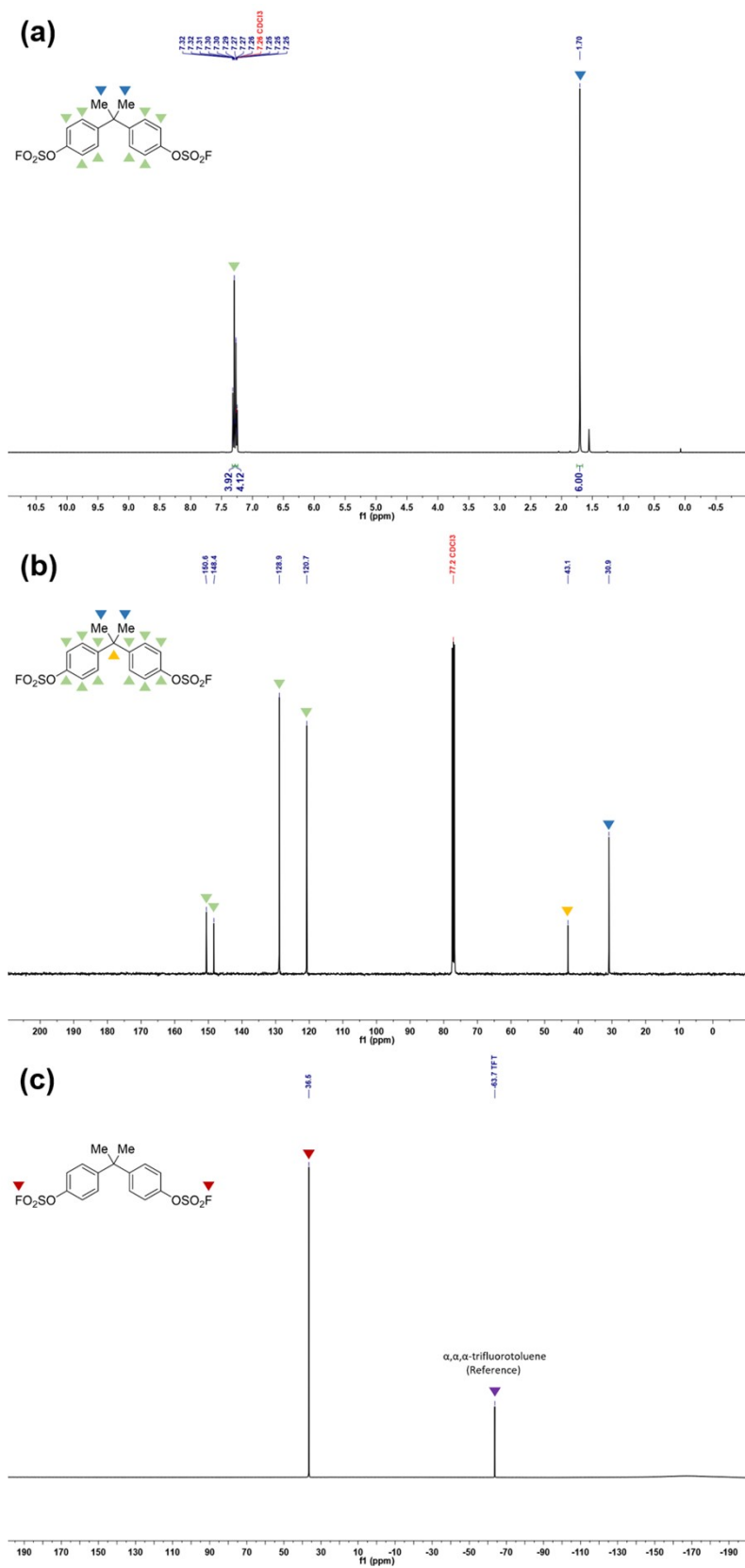


Fig.S2 (a) ^1H NMR (400 MHz, CDCl_3), (b) ^{13}C NMR (100 MHz, CDCl_3), (c) ^{19}F NMR (377 MHz, CDCl_3).

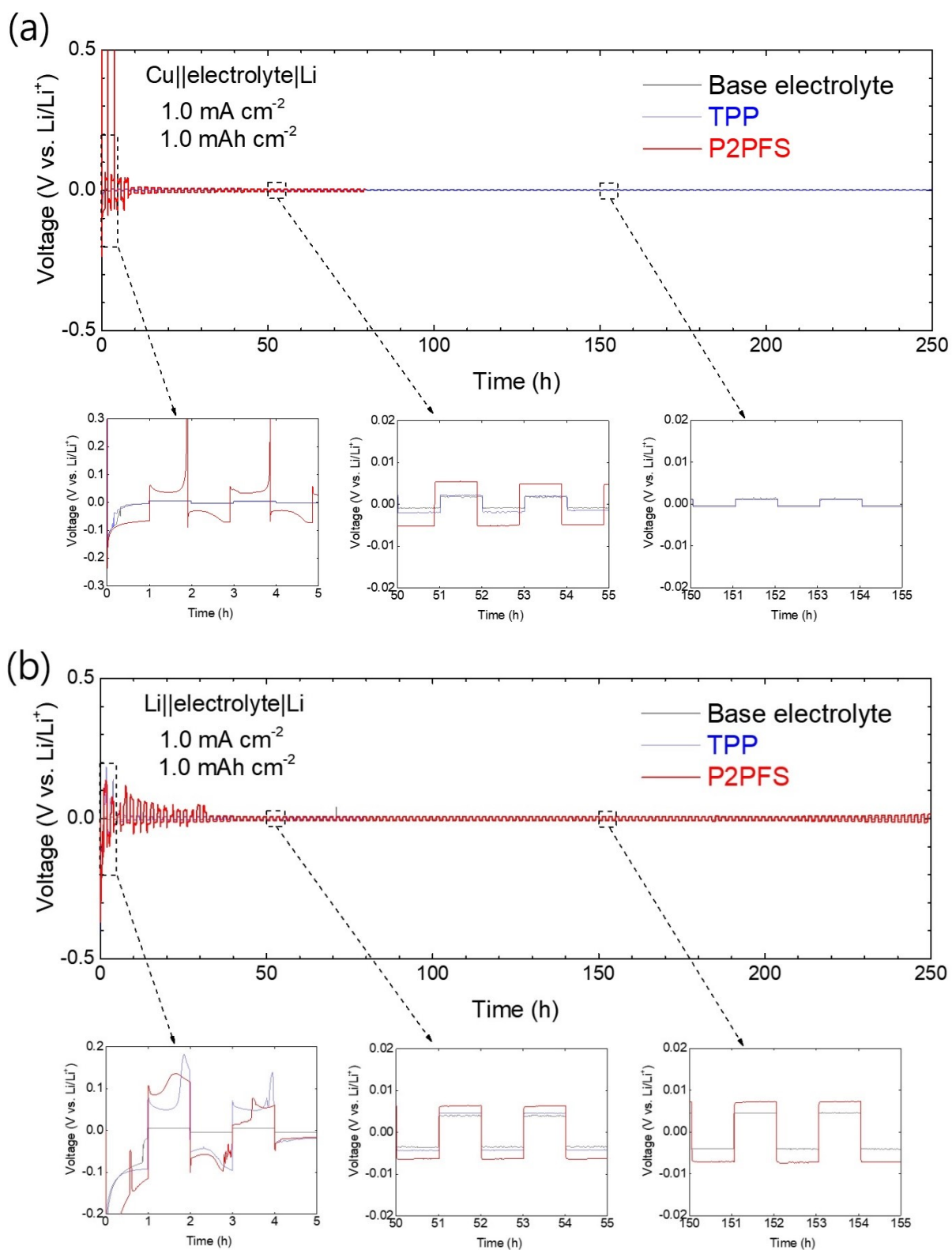


Fig.S3 Polarization behaviors of (a) Cu/Li asymmetric and (b) Li/Li symmetric cells with base, TPP-, and P2PFS-containing electrolytes.

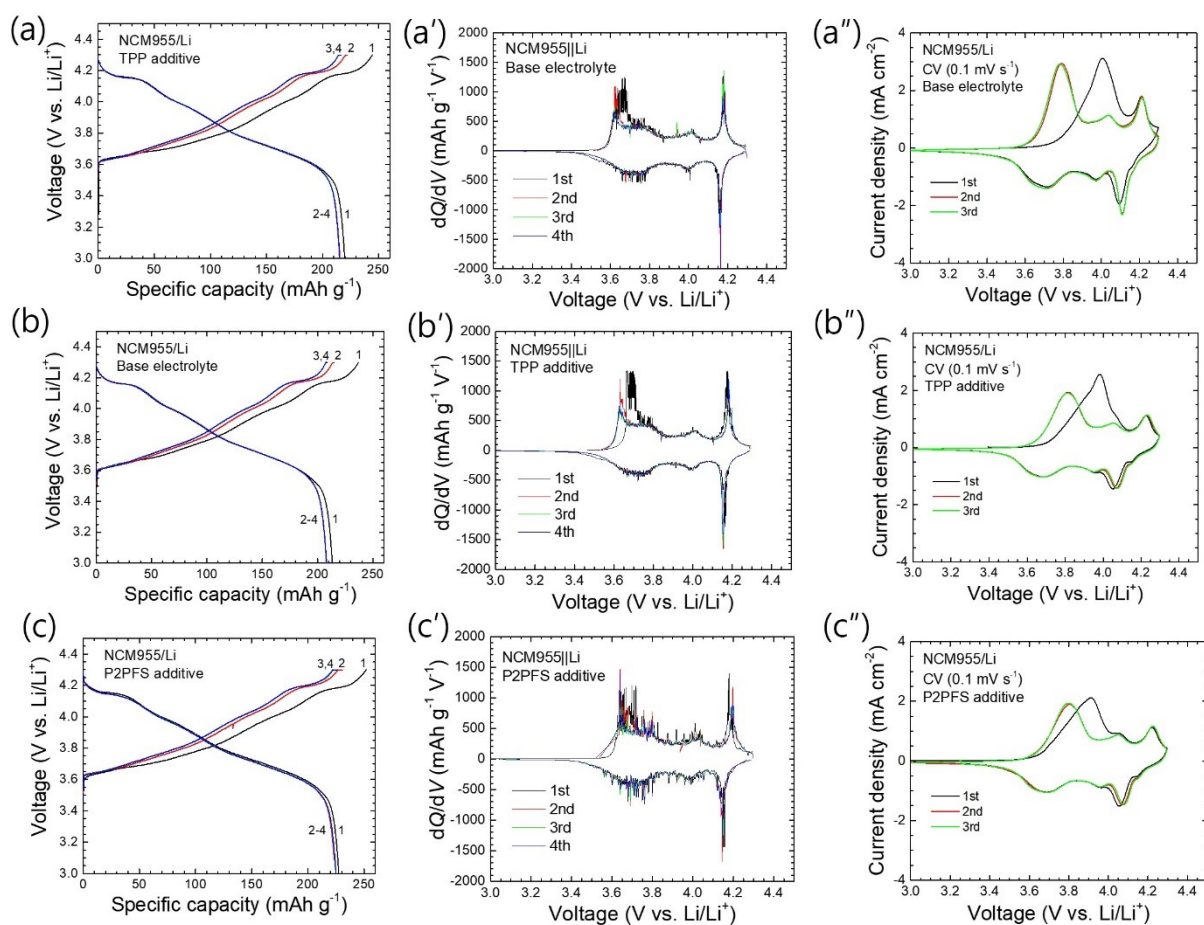


Fig.S4 Galvanostatic and potentiostatic electrochemical performance of NCM955/Li cell with base, TPP-, and P2PFS-containing electrolytes: (a,b,c) Galvanotatic charge-discharge profiles during formation at 0.1C for the first cycle and 0.2C for the consecutive 3 cycles. The numerals in the figures indicate cycle numbers; (a',b',c') dQ/dV vs. V plots calculated from (a,b,c) profiles, respectively; (a'',b'',c'') potentialstatic CV for the initial 3 cycles for the base, TPP-, and P2PFS-containing NCM955/Li cells, respectively.

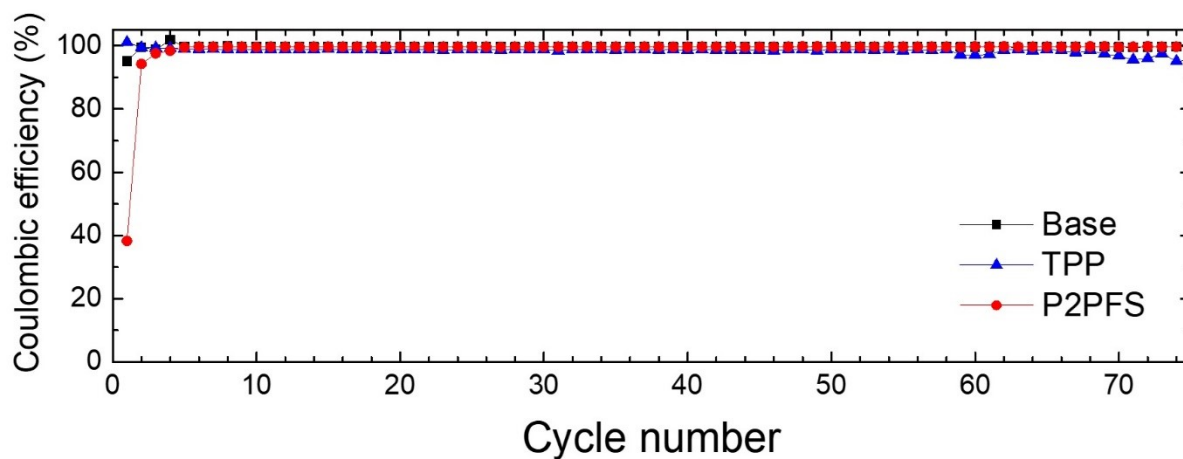


Fig.S5 Coulombic efficiency plot of Fig.3d (the cycle number is started with the first cycle at the recovered 1C process).

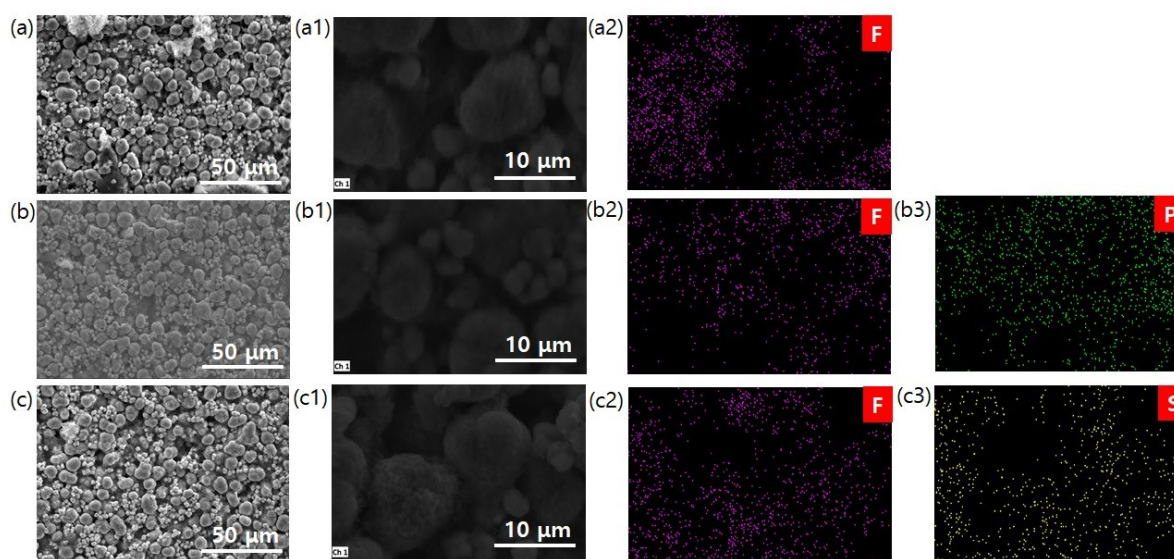


Fig.S6 SEM and EDS images of cycled NCM955 with base, TPP-, and P2PFS-containing electrolytes: (a,b,c) SEM images after various C-rate test and 1 C-rate 70 cycles; (a1,b1,c1) Magnified images of (a,b,c); (a2,b2,c2) F element distribution of (a1,b1,c1) images; (b3) P element distribution of (b1) image; (c3) S element distribution of (c1) image.

Table S1. Elements distributions of cycled NCM955 electrodes using base, TPP- and P2PFS-containing electrolytes.

Elements	Base electrolyte		TPP-containing electrolyte		P2PFS-containing electrolyte	
	Mass (%)	Error (%)	Mass (%)	Error (%)	Mass (%)	Error (%)
Ni	56.58	1.34	52.99	1.33	55.00	1.40
Co	5.38	0.19	5.26	0.20	4.80	0.18
Mn	2.52	0.11	2.33	0.11	2.41	0.11
C	14.32	2.63	20.46	3.65	17.69	3.22
O	14.14	2.08	15.30	2.43	17.53	2.64
F	4.34	0.83	1.72	0.50	2.07	0.55
P	2.42	0.13	1.76	0.11	0.19	0.04
S	0.00	0.00	0.00	0.00	0.18	0.04
Al	0.31	0.06	0.18	0.05	0.13	0.04

Reference

1. H. Haruna, S. Takahashi and Y. Tanaka, *J. Electrochem. Soc.*, 2017, **164**, A6278-A6280.